Journal of Environmental Chemical Engineering 11 (2023) 110962

Contents lists available at ScienceDirect

Journal of Environmental Chemical Engineering

journal homepage: www.elsevier.com/locate/jece

Fabrication of multi-morphological $Bi_2O_2(OH)NO_3$-$BiVO_4$ Z-Scheme heterojunction for enhanced photocatalytic antibiotic removal performance

Jinhai Li [a], Chenyu Wang [a], Jianhai Zhou [b], Zhang Ping [b], Guopei Huang [c], Yuanhui Wu [d], Shuxing Luo [d], Dongmei Bao [a], Zhu Wen [a], Pili Lu [a,*]

[a] School of Materials Science and Engineering, Guizhou Minzu University, Guiyang 550025, PR China
[b] School of Chemical Engineering, Guizhou University of Engineering Science, Bijie 551700, PR China
[c] State Key Laboratory of Environment Geochemistry, Institute of Geochemistry Chinese Academy of Sciences, Guiyang 550025, PR China
[d] Department of Chemistry and Chemical Engineering, Zunyi Normal College, Zunyi 563006, PR China

ARTICLE INFO

Editor: Javier Marugan

Keywords:
Photocatalysis
$Bi_2O_2(OH)NO_3$-$BiVO_4$
Heterojunction

ABSTRACT

Due to the suitable band gap, good stability, and convenient preparation, bismuth vanadate ($BiVO_4$) is regarded as one of potential semiconductor photocatalyst. However, the practical application was restricted by low catalytic efficiency and the poor charge separation. To address these obstacles, a novel Bi-based $Bi_2O_2(OH)NO_3$-$BiVO_4$ heterogeneous composite was constructed and synthesized by a mild and convenient hydrothermal method. The results of XRD, SEM, XPS, and DRS characterizations indicated that the $Bi_2O_2(OH)NO_3$-$BiVO_4$ heterogeneous catalyst were prepared successfully. The as-synthesized $Bi_2O_2(OH)NO_3$-$BiVO_4$ composite had good surface properties and catalytic stability. The results of photocatalytic degradation demonstrated that the tetracycline removal capacity of $Bi_2O_2(OH)NO_3$-$BiVO_4$ composite was obviously enhanced, and the highest degradation rate could reach 95% after 90 min. The results of quenching experiments revealed that both active species of·OH,·O_2^- and h^+ were involved in the $Bi_2O_2(OH)NO_3$-$BiVO_4$ catalytic system. The possible degradation pathways for tetracycline degradation were proposed by detecting the intermediate products of the degradation process using UPLC-MS technology. Under the interference of pH, common ions and organic matter in aquatic systems, the degradation system can still remain high degradation efficiency. It shows that the $Bi_2O_2(OH)NO_3$-$BiVO_4$ composite may be a promising photocatalyst for practical application. The current study provides new insight into developing more effective photocatalysts for antibiotic wastewater treatment.

1. Introduction

Nowadays, in order to prevent and treat bacterial infections and other diseases, more and more antibiotic drugs are constantly being developed and applied [1–3]. However, a lot of antibiotic drugs can't be fully absorbed, and most of them are released into the environment through the form of mother or metabolites [4,5]. The misuses of antibiotic drugs in humans and animals have led to the excessive discharge of medicinal antibiotics into the environment [6–8]. As one of broad-spectrum antibiotics, tetracycline-like drugs are extensively used in human and animals, and they are frequently detected in the aqueous environments such as rivers and lakes [9–12]. The antibiotic residues are difficult to be degraded effectively by the traditional sewage treatment process [13,14]. They could cause microbial mutation, drug resistance genes, bioaccumulation and biomagnification effects, which will lead to increase the ecological and health risks [15,16]. Therefore, it is critical to develop new methods to remove antibiotic residues from the aqueous environments.

Recently, semiconductor photocatalytic technology has been regarded as a promising advanced oxidation process for environmental remediation because of low cost, convenient operation, environmentally friendly [17–21]. Usually, organic pollutants could be oxidized into small molecular substances, which are low toxicity or nontoxic. Finally, the mothers and intermediates may be decomposed into CO_2 and H_2O. Up to present, a lot of photocatalysts have been exploited successively, such as metal oxides (TiO_2, ZnO), composite oxide ($CuAl_2O_4$, $BaTiO_3$, $BiVO_4$, and so on [22,23]. Among various semiconductors, Bi-based catalysts have attracted an increasing attention for the suitable band gap, good stability, and convenient preparation [24,25]. In the family of Bi-based catalysts, the $BiVO_4$ has three types of crystal polymorphisms

* Corresponding author.
E-mail address: 2463462628@qq.com (P. Lu).

https://doi.org/10.1016/j.jece.2023.110962
Received 1 June 2023; Received in revised form 26 July 2023; Accepted 4 September 2023
Available online 9 September 2023

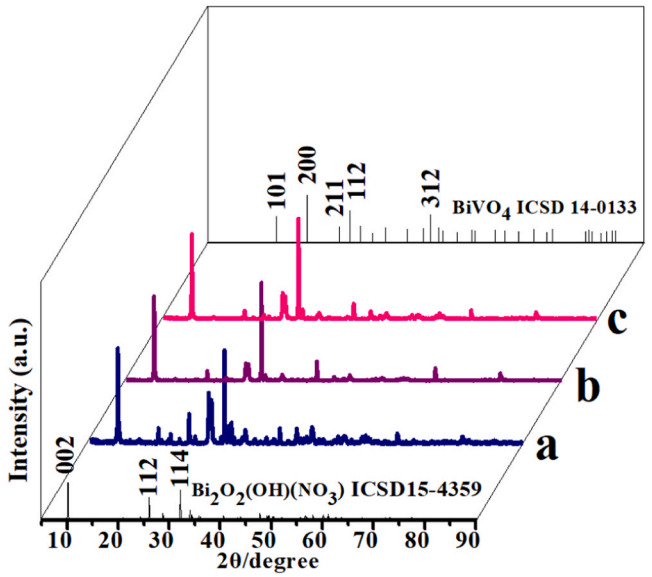

Fig. 1. XRD patterns of the as-prepared Bi-based samples under various preparation condition.

(monoclinic clinobisvanite, orthorhombic pucherite and tetragonal-dreyerite) [5]. The band gap of monoclinic clinobisvanite BiVO4 is about 2.4–2.5 eV and its responsiveness in the visible region, which is regarded as one of the most promising solar-driven photocatalyst. However, the photocatalytic efficiency is also limited by low utilization efficiency of sunlight and the poor separation of photocarriers in individual $BiVO_4$ [26–28].

Usually, constructing heterojunction is regarded as known strategy to enhance the performance of photocatalyst [29,30]. Meanwhile, the Z-scheme heterojunction photocatalyst is also regarded as an effective method for improving the spatial separation of photo-generated charge carriers, and many studies have been reported such as $SrTiO_3$-$BiVO_4$, g-C_3N_4-TiO_2 and so on[31–33]. However, the Z-scheme heterostructure of $Bi_2O_2(OH)NO_3$-$BiVO_4$ has not been reported in the literature. Based on the prior studies, the conduction band (CB) and valence band (VB) of $Bi_2O_2(OH)NO_3$ can be well match with the corresponding band of $BiVO_4$ [34–36]. Therefore, a wide-spectra-responsive Z-scheme system of $Bi_2O_2(OH)NO_3$-$BiVO_4$ was constructed firstly, which was synthesized by a mild and convenient hydrothermal method. It was expected that the heterostructure could be effectively constructed between $Bi_2O_2(OH)NO_3$ and $BiVO_4$, and the separation efficiency of photogenerated carriers can be accelerated by the heterogeneous interfaces of the $Bi_2O_2(OH)NO_3$/$BiVO_4$ composites. Furthermore, under simulated solar light irradiation, the photocatalytic degradation performance of tetracycline will be studied in detail, such as phase composition, morphological structure and photochemical properties. The possible removal pathways of tetracycline are also investigated systematically by the results of high performance liquid chromatography with mass-spectrometric detection (HPLC-MS). Moreover, the toxicity of tetracycline and the photodegradation intermediates were also investigated. The current work would inject a new strategy to develop novel photocatalysts for antibiotics wastewater treatment, and the findings are also anticipated to deeply understand the possible photochemical behavior of tetracycline in the aqueous environment.

2. Materials and methods

2.1. Chemicals

Tetracycline hydrochloride (TC), humic acid (HA), Bismuth nitrate ($Bi(NO_3)_3{\cdot}5\ H_2O$), nitric acid (HNO_3), sodium hydroxide (NaOH), Magnesium chloride ($MgCl_2{\cdot}6\ H_2O$), Calcium chloride($CaCl_2$), sodium chloride (NaCl), sodium dihydrogen phosphate (NaH_2PO_4), Acetic acid (CH_3COOH), sodium hydrogen carbonate ($NaHCO_3$), and other chemicals were supplied by Sinopharm Chemical Reagent Co., Ltd. (SCRC, Shanghai, China). All reagents were analytical purity or higher, and they were used without further purification.

2.2. Synthesis

The $Bi_2O_2(OH)NO_3$/$BiVO_4$ composites were synthesized by mild hydrothermal method at given pH values. Firstly, a certain weight of Bi $(NO_3)_3{\cdot}5\ H_2O$ and NH_4VO_3 was respectively dissolved 2 mol/L of aqueous sodium hydroxide and dilute nitric acid at magnetic stirring for 0.5 h to dissolve the raw materials. The pH values of the mixture were adjusted by the aqueous sodium hydroxide and dilute nitric acid. Next, they were transferred into a 100 mL Teflon-lined autoclave and sealed tightly. Then, the autoclaves were heated at 180 °C for 24 h. Subsequently, the autoclaves were naturally cooled to room temperature. The solid-liquid mixtures were centrifuged, and the solid products were alternately washed three times with anhydrous ethanol and deionized water. The final samples were dried at 80 °C. A series of $Bi_2O_2(OH)NO_3$/$BiVO_4$ samples were prepared by changing the molar ratio of $Bi(NO_3)_3{\cdot}5\ H_2O$ to NH_4VO_3. Meanwhile, the pure $Bi_2O_2(OH)NO_3$ and $BiVO_4$ were also synthesized respectively under the same conditions.

2.3. Characterization

An X-ray diffractometer (XRD, Empyrean) was used to detect the as-prepared Bi-based photocatalysts. A field-scanning electron microscope (Nova Nano FESEM 450) and a transmission electron microscope (TEM, Tecnai G2 F20 S-TWIN) were employed to measure the morphology of the synthesized Bi-based samples. The surface composition and chemical state of the as-prepared Bi-based samples were studied by an X-ray photoelectron spectroscopy (XPS, PHI5000V). The UV–vis diffuse reflectance spectra (UV–vis DRS) of the synthesized Bi-based samples were recorded on a UV–Vis spectrophotometer (SolidSpec-3700). The surface area of the samples was recorded on a BET ASAP 2020 micrometrics instrument. A CHI-660E electrochemical workstation (CH Instruments, Shanghai, China) was employed to measure electrochemical impedance spectroscopy (EIS). The concentration of tetracycline and the intermediates formed during the photocatalytic degradation process was monitored on an ultra-high performance liquid chromatography–high resolution mass spectrometry (UHPLC- HRMS, Ultimate3000 and Q Exactive).

2.4. Photocatalytic experiment

The photocatalytic tetracycline degradation tests were conducted in a reactor (BL-GHX-V) purchased from Shanghai Bilang Instrument Co., Ltd (Shanghai, China). A 300 W Xenon arc lamp was used as simulated solar light source during the photocatalytic degradation process. In a typical experimental procedure, 50 mg of as-prepared Bi-based photocatalyst and 100 mL aqueous solution of tetracycline (10 mg/L) was added into the quartz photoreactor. Subsequently, the suspension was magnetically stirred and adequately dispersed in the dark for 0.5 h to establish an adsorption–desorption equilibrium between the Bi-based photocatalyst and tetracycline. Then the reaction system was illuminated with simulated solar light. At certain time intervals, 5 mL of the suspension was sampled and filtrated through a 0.22 μm Millipore membrane to remove the solid particles. The concentrations of tetracycline and the degradation intermediates were analyzed using an ultra-high performance liquid chromatography mass spectrometry. The removal efficiency of tetracycline was recorded as R, which was calculated by the following equation [37]:

$$R = (C_0–C_t)/C_0\times 100\% \quad (1)$$

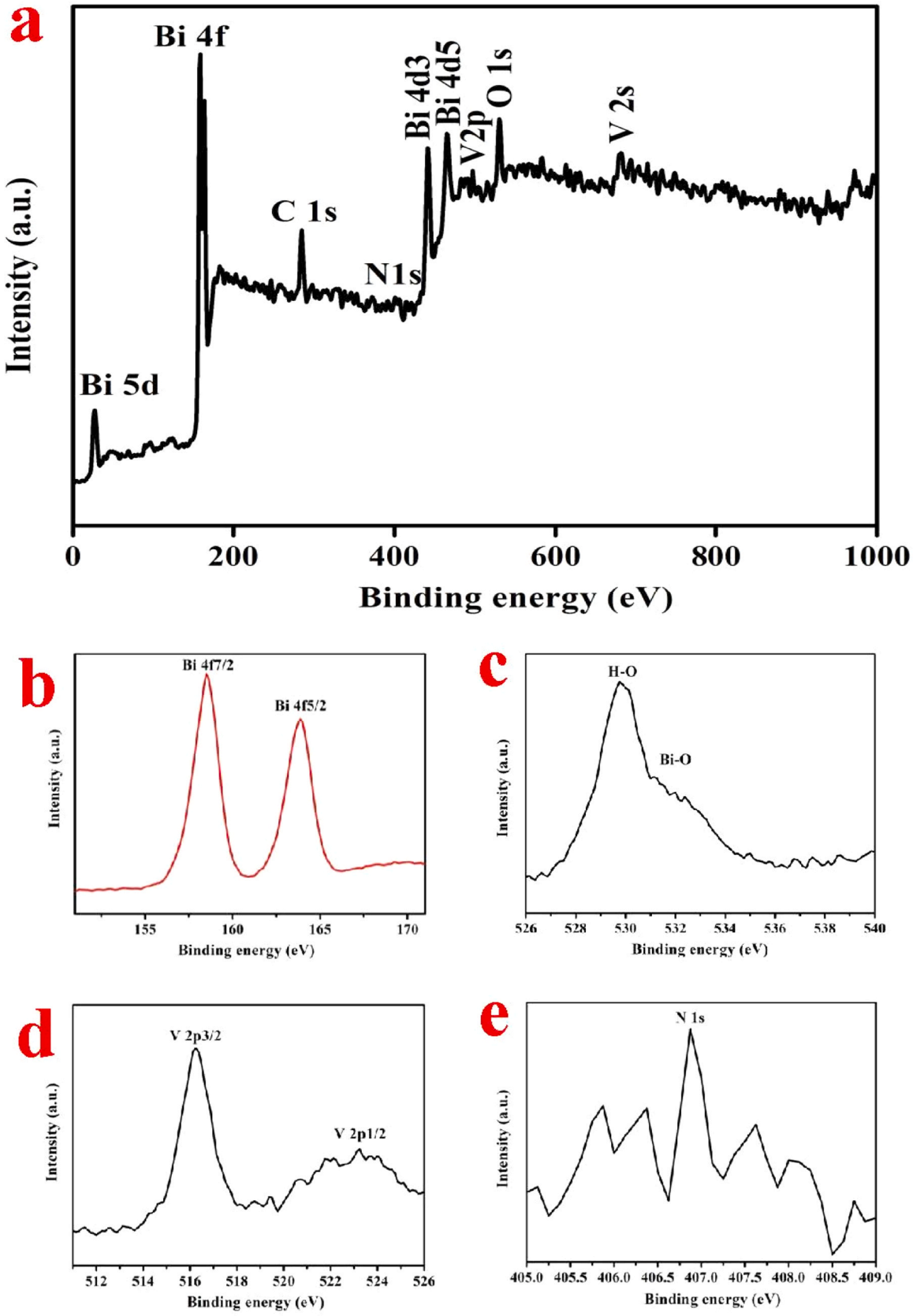

Fig. 2. XPS spectra of $Bi_2O_2(OH)NO_3/BiVO_4$ (3:1), (a) XPS fully survey spectra, (b) Bi4f, (c) O1s, (d) V2p and (e) N1s.

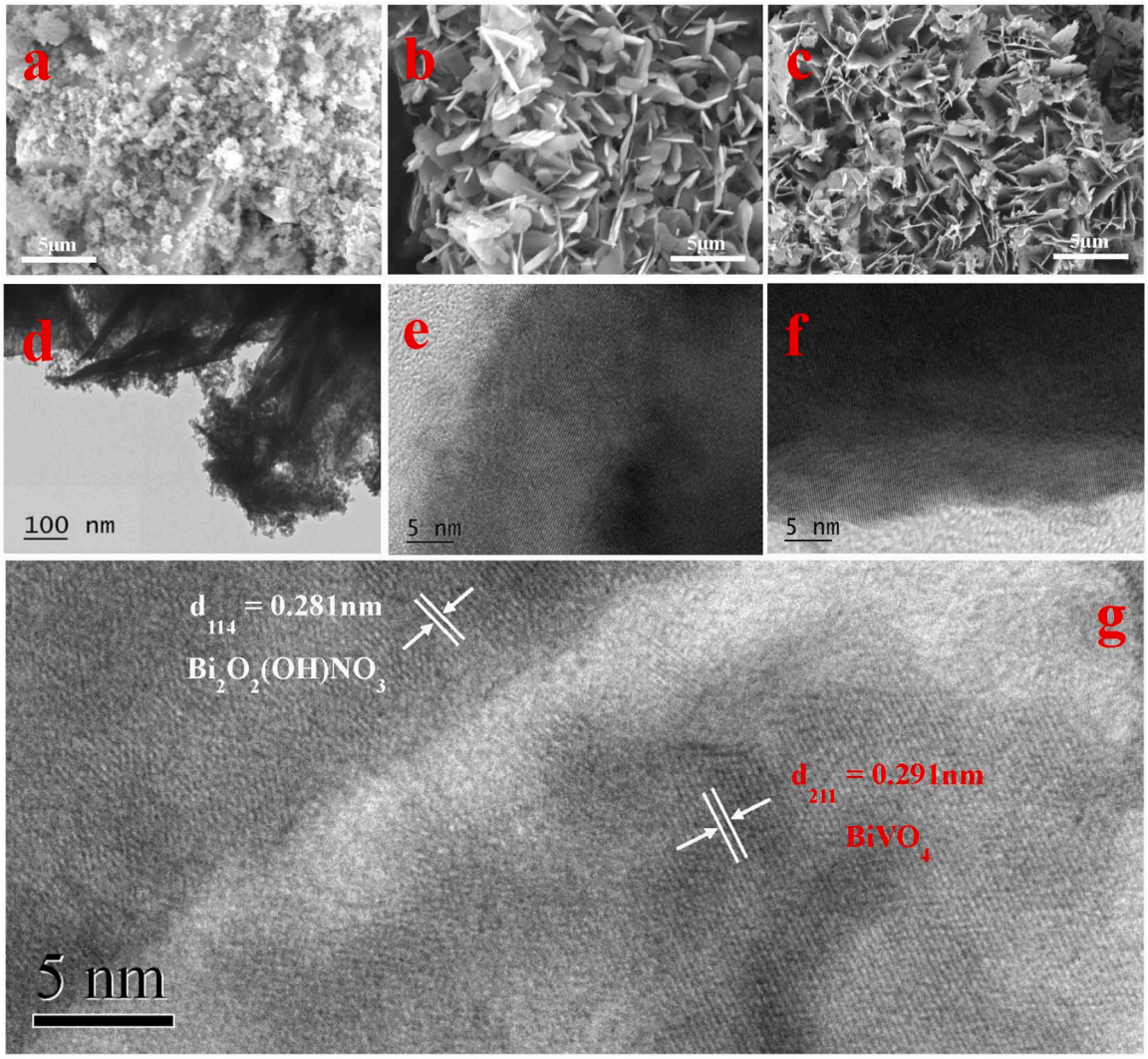

Fig. 3. SEM images (a, b, c) of $Bi_2O_2(OH)NO_3$, $BiVO_4$, and $Bi_2O_2(OH)NO_3/BiVO_4$, TEM image (d) of $Bi_2O_2(OH)NO_3/BiVO_4$, HRTEM images (e, f, g) of $Bi_2O_2(OH)NO_3$, $BiVO_4$, and $Bi_2O_2(OH)NO_3/BiVO_4$.

Where the C_0 represents the initial concentration of tetracycline, and C_t means the concentration of tetracycline at a given irradiated time interval. Moreover, the effect of photocatalytic reaction factors were also investigated, included the pH (5, 7 and 9), and the effects of Na^+, Ca^{2+}, Mg^{2+}, Cl^-, NO_3^-, SO_4^{2-}, $H_2PO_4^-$, HCO_3^-, CH_3COO^-, HA, SA and AC were also studied. In addition, the recycling experiments and the natural control experiments were carried respectively.

2.5. Toxicity assessment

The toxicity of tetracycline and its degradation intermediates were evaluated through the ECOSAR prediction model. It was developed by the U.S. Environmental Protection Agency. Three aquatic species of fish, daphnid, and algae were involved mainly, and the corresponding median lethal (96 h or 48 h LC50), median effective concentration (96 h EC50), and chronic value (ChV) was investigated.

3. Results and discussions

3.1. Structure and morphology

The crystalline phase of the as-prepared Bi-based samples was examined by XRD patterns. The XRD pattern of $Bi_2O_2(OH)NO_3/BiVO_4$ composites were shown in Fig. 1. The $Bi_2O_2(OH)NO_3/BiVO_4$ composites were in the mole ratio of 2:1, 3:1 and 4:1 of $Bi_2O_2(OH)NO_3$ and $BiVO_4$ labeled as a, b and c respectively. It can be seen that the diffraction peaks of the Bi-based composties at 18.32°, 24.37°, 32.68°, 48.40° corresponds well to the crystal planes of (101), (200), (112), and (312) of $BiVO_4$ (ICSD 14–0133), respectively [38]. Meanwhile, the diffraction peaks of the as-prepared samples at 10.31°, 25.55° and 31.29° matches well with its (002), (112) and (114) crystal planes of $Bi_2O_2(OH)NO_3$ (ICSD 15–4359) accordingly [39]. Which suggested that the diffraction peaks of pure $Bi_2O_2(OH)NO_3$ and that of $BiVO_4$ were all retained in the as-prepared samples and indicated the coexistence of $Bi_2O_2(OH)NO_3$ and $BiVO_4$. It was confirmed that the $Bi_2O_2(OH)NO_3/BiVO_4$ composites were prepared successfully.

The composition and chemical state of the as-prepared $Bi_2O_2(OH)NO_3/BiVO_4$ composite $Bi_2O_2(OH)NO_3/BiVO_4$ composite (with the 3:1 mol ratio of $Bi_2O_2(OH)NO_3$ to $BiVO_4$) was studied by XPS analysis. As shown in Fig. 2a, the survey spectrum of the as-prepared Bi-based sample revealed that all of the detected elements were well matched with their composition in the composite. The C 1 s peak of the adventitious carbon was also detected in the spectrum, which may be caused by the XPS instrument and dust in the environment. The high resolution spectra of Bi 4 f, O2s, N 1 s and V2p were also found availably. As shown in Fig. 2b, two peaks of the high resolution XPS spectrum of Bi 4 f were observed. They were located at 158.5 and 164.5 eV, which can be corresponded to the binding energies of Bi 4f7/2 and Bi 4f5/2, respectively.

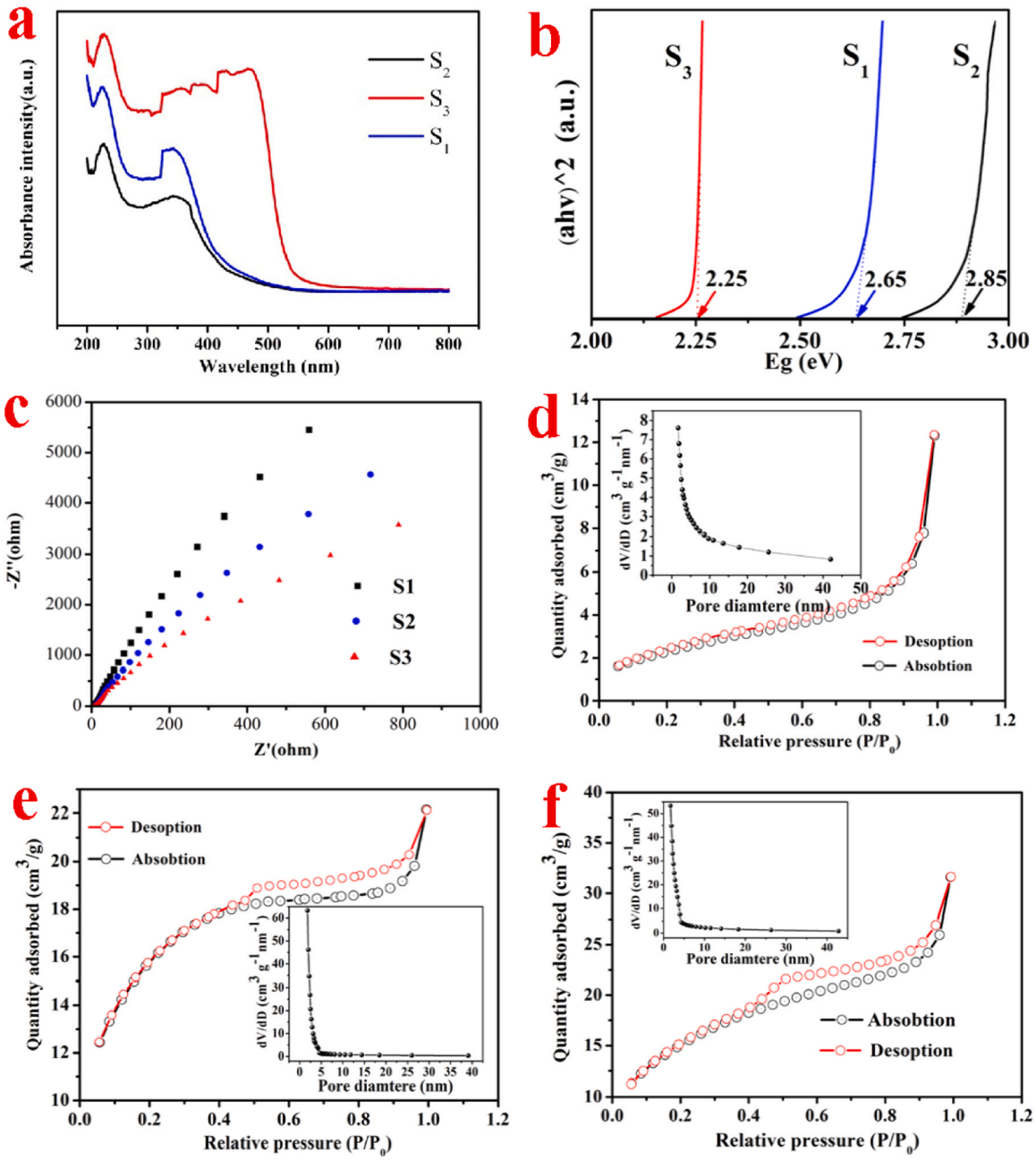

Fig. 4. (a) the UV–vis diffuse reflection spectra of the as-prepared samples, (b) the band gaps of the as-prepared samples, (c) the electrochemical impedance spectroscopy (EIS) Nyquist plots of the as-prepared samples, (d-f)Nitrogen adsorption-desorption isotherms and pore size distribution curves of the as-prepared samples.

They were characteristic peaks of Bi^{3+} [40], which exhibited the presence of Bi^{3+} in the as-prepared composite. Fig. 2c showed the O 1 s spectrum could be deconvoluted into two peaks. One located at 529.9 eV could be ascribed to the Bi-O chemical bond. The other located at 532.0 eV, which can be assigned to H-O in $Bi_2O_2(OH)(NO_3)$ [41,42]. Fig. 2d was the high-resolution XPS spectra of V2p, the binding energies of V2p3/2 and V2p1/2 were 516.3 and 523.3 eV, which can be corresponded to the V^{5+}. Fig. 2e showed that the N 1 s spectra of the sample, the peak centered at 407.6 eV can be assigned to NO_3^-. The XPS analysis of the sample further proved that the $Bi_2O_2(OH)NO_3/BiVO_4$ composite was synthesized successfully.

The morphology and microstructure of the as-prepared Bi-based samples were checked by SEM, TEM and HRTEM, which were presented in Fig. 3. Fig. 3a showed that the pure $Bi_2O_2(OH)NO_3$ samples were stacked by many nano-particles. Obviously, the as-prepared $BiVO_4$ samples were constituted by uniform flowerlike hierarchical microstructures (Fig. 3b). TEM images of $Bi_2O_2(OH)NO_3/BiVO_4$ composite (Fig. 3c) revealed that the co-existence of nano-particle $Bi_2O_2(OH)NO_3$ and the aggregation of $BiVO_4$ hierarchical microstructure. The HRTEM image was detected to further observe the heterojunction structure between $Bi_2O_2(OH)NO_3$ and $BiVO_4$. Fig. 3d displayed that the $BiVO_4$ sheets were intimately contacted by $Bi_2O_2(OH)NO_3$ particles.

The high-resolution TEM (HRTEM) images of $Bi_2O_2(OH)NO_3$, $BiVO_4$, and $Bi_2O_2(OH)NO_3/BiVO_4$ were presented in Fig. 3e, Fig. 3f, Fig. 3g respectively. As shown in Fig. 3g, an interface transition zone can be observed obviously, which was similar with Fig. 3e and Fig. 3f. Meanwhile, Fig. 3g exhibited the lattice fringe with a spacing of 0.281 nm corresponded well to the (114) plane of $Bi_2O_2(OH)NO_3$, and the

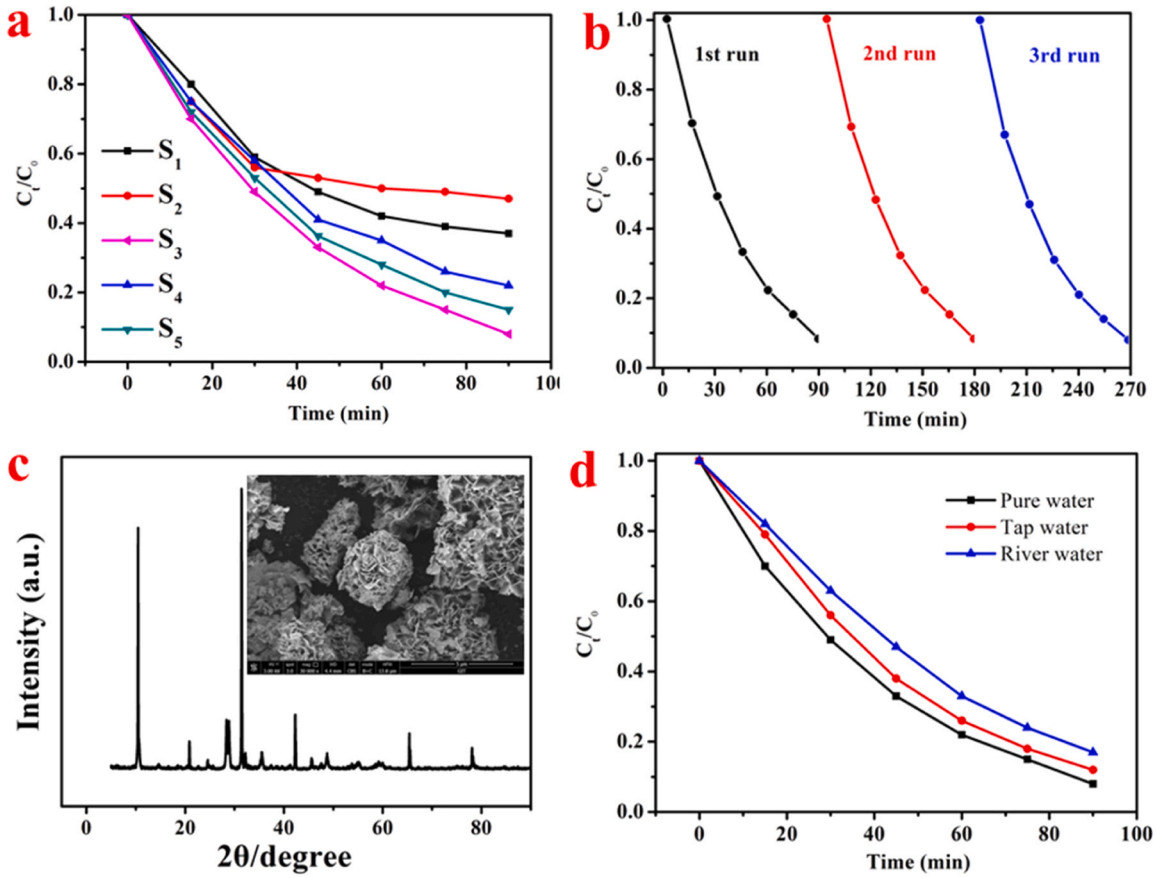

Fig. 5. (a) the degradation curves of tetracycline, (b) cycling test, (c) the XRD patterns and SEM images of the reused $Bi_2O_2(OH)NO_3/BiVO_4$ composite, (d) water quality conditions.

measured interplanar distances of 0.291 nm matched with D-spacing of the (211) crystal of $BiVO_4$ [39]. The results of the TEM and HRTEM analyses portended that the separation and transfer of photoinduced charge carries maybe accelerated by the intimate heterojunction structure between $Bi_2O_2(OH)NO_3$ and $BiVO_4$ in $Bi_2O_2(OH)NO_3/BiVO_4$ composite.

3.2. DRS analysis

The light absorption properties of as-prepared Bi-based samples were studied by investigating the UV–vis diffuse reflection spectra (UV–vis DRS). As shown in Fig. 4a (the abbreviations S1, S2 and S3 mean $Bi_2O_2(OH)NO_3$, $BiVO_4$ and $Bi_2O_2(OH)NO_3/BiVO_4$ respectively), $Bi_2O_2(OH)NO_3/BiVO_4$ composite has strong absorption of ultraviolet and visible light. The light absorption of $Bi_2O_2(OH)NO_3/BiVO_4$ was enhanced by the heterojunction effect between $Bi_2O_2(OH)NO_3$ and $BiVO_4$. Furthermore, $Bi_2O_2(OH)NO_3/BiVO_4$ composite can observe an obvious red-shift compared with $Bi_2O_2(OH)NO_3$ and $BiVO_4$. Meanwhile, the values of band gap of as-prepared Bi-based samples were quantitatively estimated by the Kubelka-Munk approach:

$$\alpha h\nu = A(h\nu - E_g)^{n/2} \quad (2)$$

Where α is the optical absorption coefficient, the Eg is band gap, A is a constant and hν, and hν is photonic energy. As $Bi_2O_2(OH)NO_3$ and $BiVO_4$ are both indirect semiconductors [38], n is 4 for them. Based on the $(\alpha h\nu)^{1/2}$ versus (hν) plot in Fig. 4b, which indicated that the optical band gap of $Bi_2O_2(OH)NO_3/BiVO_4$ is 2.25 eV, and the Eg values of $Bi_2O_2(OH)NO_3$ and $BiVO_4$ were 2.65 eV and 2.85 eV respectively. It suggested that $Bi_2O_2(OH)NO_3/BiVO_4$ composite had a smaller optical band gap structure, which meant that the composite had a greater response of under the irradiation of sunlight, and its photocatalytic performance maybe improved. Meanwhile, this result was also confirmed by the electrochemical impedance spectra (EIS) measurement. As shown in Nyquist plot (Fig. 4b), which indicated that the $Bi_2O_2(OH)NO_3/BiVO_4$ had a smaller arc radius than both $Bi_2O_2(OH)NO_3$ and $BiVO_4$. It revealed that the formation of Z-scheme heterostructure of $Bi_2O_2(OH)NO_3/BiVO_4$ can effectively promote the separation of photogenerated carriers and fast charge transfer. Furthermore, to investigate the influence factor of the photoresponse property, the specific surface area was determined by the Nitrogen adsorption-desorption isotherms. The results were presented in Fig. 4d-f. Where, d, e and f meant $Bi_2O_2(OH)NO_3$, $BiVO_4$ and $Bi_2O_2(OH)NO_3/BiVO_4$ respectively, and their specific surface areas were 1.70 m^2g^{-1}, 2.99 m^2g^{-1}, 5.20 m^2g^{-1} respectively. Obviously, the specific surface area of $Bi_2O_2(OH)NO_3/BiVO_4$ composite was larger than granular $Bi_2O_2(OH)NO_3$ and flaky $BiVO_4$. Combining the results of DRS analysis and EIS measurement, the excellent response performances of $Bi_2O_2(OH)NO_3/BiVO_4$ composite could be attributed to its larger specific surface area Z-scheme heterostructure, and the enhanced photocatalytic activity had been further verified by the result of photocatalytic degradation experiment.

3.3. Photocatalytic performance

To investigate the activities of as-prepared Bi-based samples, the experiments of photocatalytic degradation were measured in a liquid–solid reaction system under simulated solar light radiation. Firstly, the photocatalytic activity of the $Bi_2O_2(OH)NO_3$, $BiVO_4$ and $Bi_2O_2(OH)NO_3/BiVO_4$ composite was evaluated by measuring the degradation of tetracycline. As shown in Fig. 5a (the abbreviations S1 and S2 mean $Bi_2O_2(OH)NO_3$ and $BiVO_4$, the $Bi_2O_2(OH)NO_3/BiVO_4$ composites were

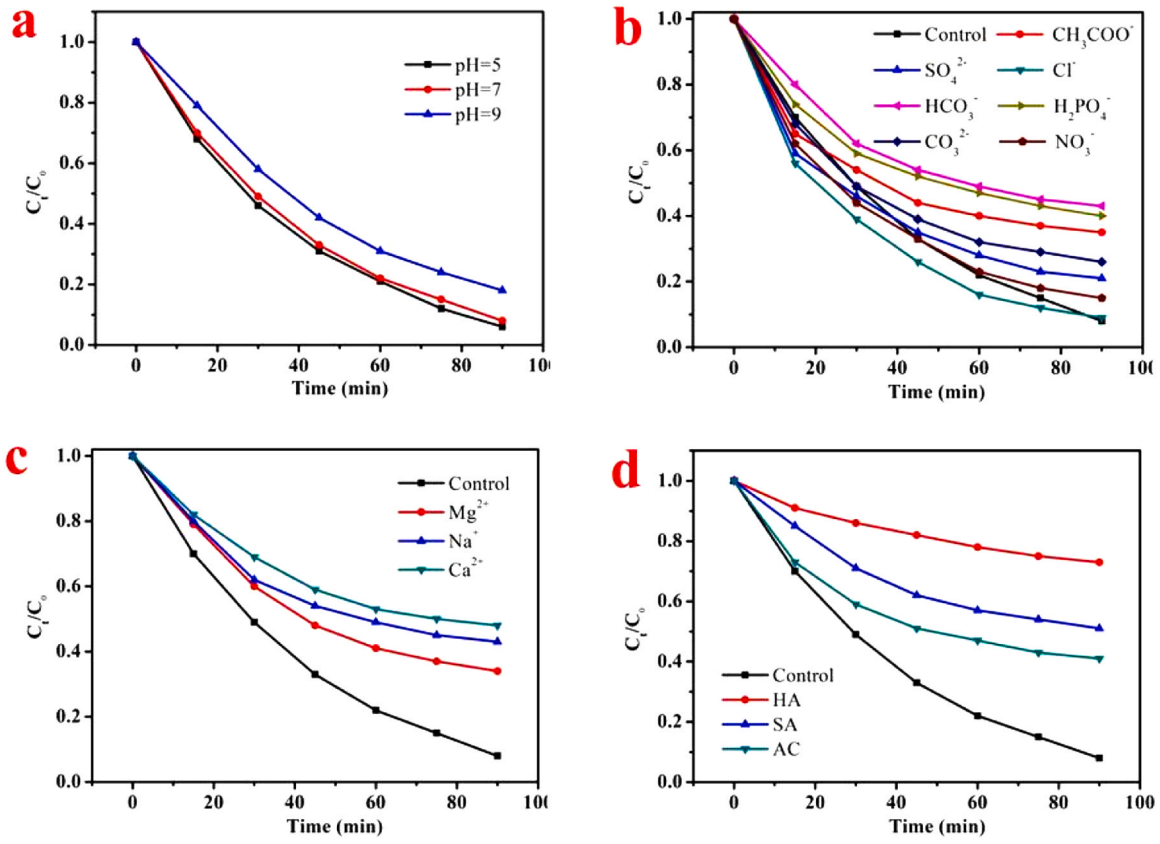

Fig. 6. Removal efficiencies of tetracycline with different (a) pH values; (b) anions; (c) cations; (d) concentrations of organic materials.

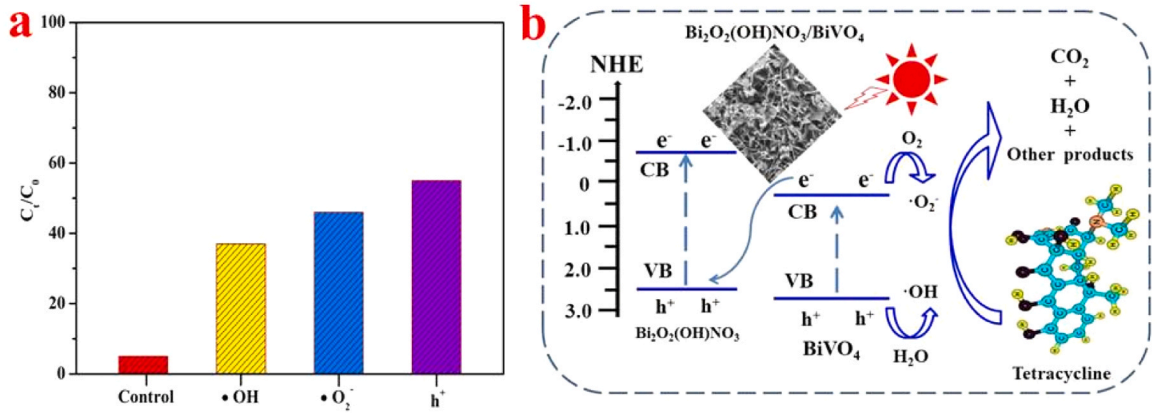

Fig. 7. (a) Effect of different quenchers on tetracycline degradation in $Bi_2O_2(OH)NO_3$-$BiVO_4$ system; (b) Proposal mechanism of tetracycline degradation in $Bi_2O_2(OH)NO_3$-$BiVO_4$ photocatalytic system.

in the mole ratio of 2:1, 3:1 and 4:1 of $Bi_2O_2(OH)NO_3$ and $BiVO_4$ labeled as S4, S3 and S5 respectively), $Bi_2O_2(OH)NO_3$ and $BiVO_4$ exhibited weak photocatalytic performance. The $Bi_2O_2(OH)NO_3/BiVO_4$ (3:1) composite displayed greatly improved photocatalytic degradation, where about 95% of tetracycline was photodegraded under the same conditions. The reusability and stability of as-prepared $Bi_2O_2(OH)NO_3/BiVO_4$ photocatalyst was used in three repeat tetracycline degradation experiments, and the photocatalyst was characterized by XRD and SEM. As shown in Fig. 5b, the rate of tetracycline degradation decreased slightly after three runs, which indicated that the stability of the as-prepared $Bi_2O_2(OH)NO_3/BiVO_4$ photocatalyst was very good. As displayed in Fig. 5c, the XRD patterns and SEM images of the as-prepared $Bi_2O_2(OH)NO_3/BiVO_4$ composite photocatalyst were almost the same as those of the pristine features. Which revealed that the as-prepared $Bi_2O_2(OH)NO_3/BiVO_4$ composite photocatalyst had a good application prospect. Furthermore, the effects of water environment on tetracycline photocatalytic degradation were also investigated by sampling of different water sources (river water and tap water). Fig. 5d showed that the degradation efficiencies tap water and river water were lower than that of in distilled water. Obviously, tetracycline degradation can be restrained in real water. In references, it maybe relate with the coexisting inorganic ions and organic species in water environment [43]. Secondly, to study the influences of the coexisting materials, the influences of initial pH on tetracycline photocatalytic were investigated at different pH conditions. From Fig. 6a, a slight variation of tetracycline degradation was observed when the pH increased from 5 to 7, and an

Table 1
the brief information of tetracycline and the transformation products.

No.	*m/z*	Formula	Chemical structure
TC	445	$C_{22}H_{24}N_2O_8$	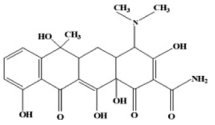
P1–1	396	$C_{20}H_{16}N_2O_7$	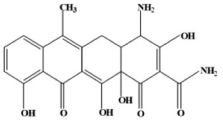
P1–2	302	$C_{17}H_{17}NO_5$	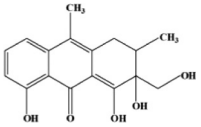
P1–3	245	$C_{13}H_{10}O_6$	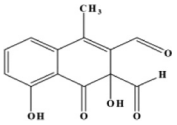
P1–4	166	$C_5H_{10}O_6$	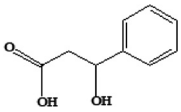
P1–5	118	$C_4H_6O_4$	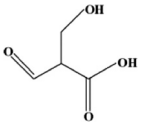
P2–1	368	$C_{20}H_{17}NO_6$	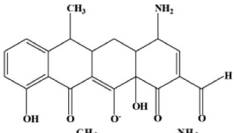
P2–2	339	$C_{19}H_{17}NO_5$	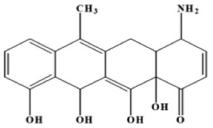
P2–3	326	$C_{19}H_{18}O_5$	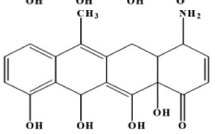
P2–4	245	$C_{14}H_{12}NO_4$	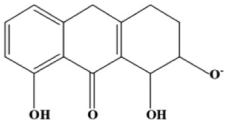
P2–5	219	$C_{13}H_{14}NO_3$	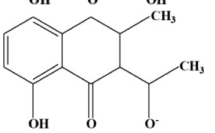
P3–1	396	$C_{20}H_{14}NO_8$	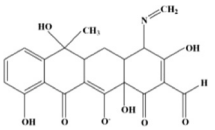
P3–2	302	$C_{16}H_{13}O_6$	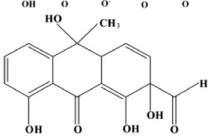
P3–3	282	$C_{14}H_{13}O_6$	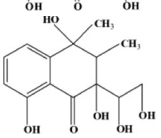

Table 1 (*continued*)

No.	*m/z*	Formula	Chemical structure
P3–4	234	$C_{12}H_{10}O_5$	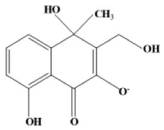
P3–5	124	$C_7H_9O_2$	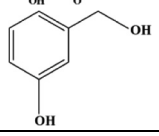

evident decrease in tetracycline degradation at pH of 9. Therefore, the pH conditions in the subsequent experimental treatments were selected as the values of 7, which further approached to the pH of the actual water environment. To study the influences of coexisting inorganic ions (Cl^-, SO_4^{2-}, $H_2PO_4^-$, NO_3^-, CO_3^{2-}, HCO_3^-, and CH_3COO^-, Mg^{2+}, Na^+ and Ca^{2+}) on tetracycline photocatalytic degradation, the corresponding experiments were systematically investigated under established experimental conditions. Fig. 6b revealed that the influences of inorganic anions were gradually increased in sequence of HCO_3^-, $H_2PO_4^-$, CH_3COO^-, CO_3^{2-}, SO_4^{2-}, NO_3^- and Cl^-. The Cl^- exhibited a slight gain effect on tetracycline degradation, because it could be transformed and generated to Cl_2 and HOCl [44]. The NO_3^- and SO_4^{2-} demonstrated in a similar effect for degradation of tetracycline. The formation of NO_3^- and SO_4^{2-} species can generate other active species, which could promote the degradation reactions of tetracycline at the beginning of the reactions. With the consumption of NO_3^- and SO_4^{2-}, the degradation reactions were suppressed gradually. However, the addition of HCO_3^-, $H_2PO_4^-$, CH_3COO^-, CO_3^{2-}, can greatly inhibit the degradation of tetracycline. These species can deplete or hinder the active species, and the pH values of reaction system could also be increased. Meanwhile, Fig. 6c revealed that the degradation of tetracycline could be inhibited by the coexisting cations of Na^+, Mg^{2+} and Ca^{2+}. Due to they can combine with tetracycline to form coordination compounds [45].

As well known, main organic matters were found in the natural water environment such as humic acid (HA). To investigate the effects of coexisting organics, humic acid (HA), salicylic acid (SA), acetic acid (AC) were added into the reaction systems. Fig. 6d showed that the addition of HA, SA, SA can greatly inhibit the degradation of tetracycline. The radicals (•OH and the others) could be consumed by the coexisting organic matters, and the degradation rate of organic pollutants could also be slowed down.

3.4. Photocatalytic mechanism

Based on above discussion and reference research, the possible mechanism of $Bi_2O_2(OH)NO_3/BiVO_4$ photocatalytic system was deduced and proposed. It was reported that the conduction band and valence band of $Bi_2O_2(OH)NO_3$ were about − 0.88 eV and 2.46 eV respectively [46]. They were higher than that of $BiVO_4$ ($E_{CB} \approx 0.32$ eV, $E_{VB} \approx 2.67$ eV) [47]. Based on literature research [48], because the CB of $Bi_2O_2(OH)NO_3$ (−0.88 eV) is more negative than the standard redox potential of $O_2/\bullet O_2^-$ (−0.33 eV), $Bi_2O_2(OH)NO_3/BiVO_4$ can obey a direct Z-scheme. An intimate and effective heterojunction can be formed by coupling with $Bi_2O_2(OH)NO_3$ and $BiVO_4$. When photons of energy higher than the band gap were harvested by semiconductors of $Bi_2O_2(OH)NO_3$ and $BiVO_4$, electrons were excited from the valence band to the conduction band and photogenerated e^-/h^+ couples were produced simultaneously. Meanwhile, the recombination of photogenerated carriers could be effectively inhibited by the formation of heterojunction between $Bi_2O_2(OH)NO_3$ and $BiVO_4$. Therefore, the photocatalytic activity of the as-prepared $Bi_2O_2(OH)NO_3/BiVO_4$ can be also enhanced substantially. To further ascertain the main active species

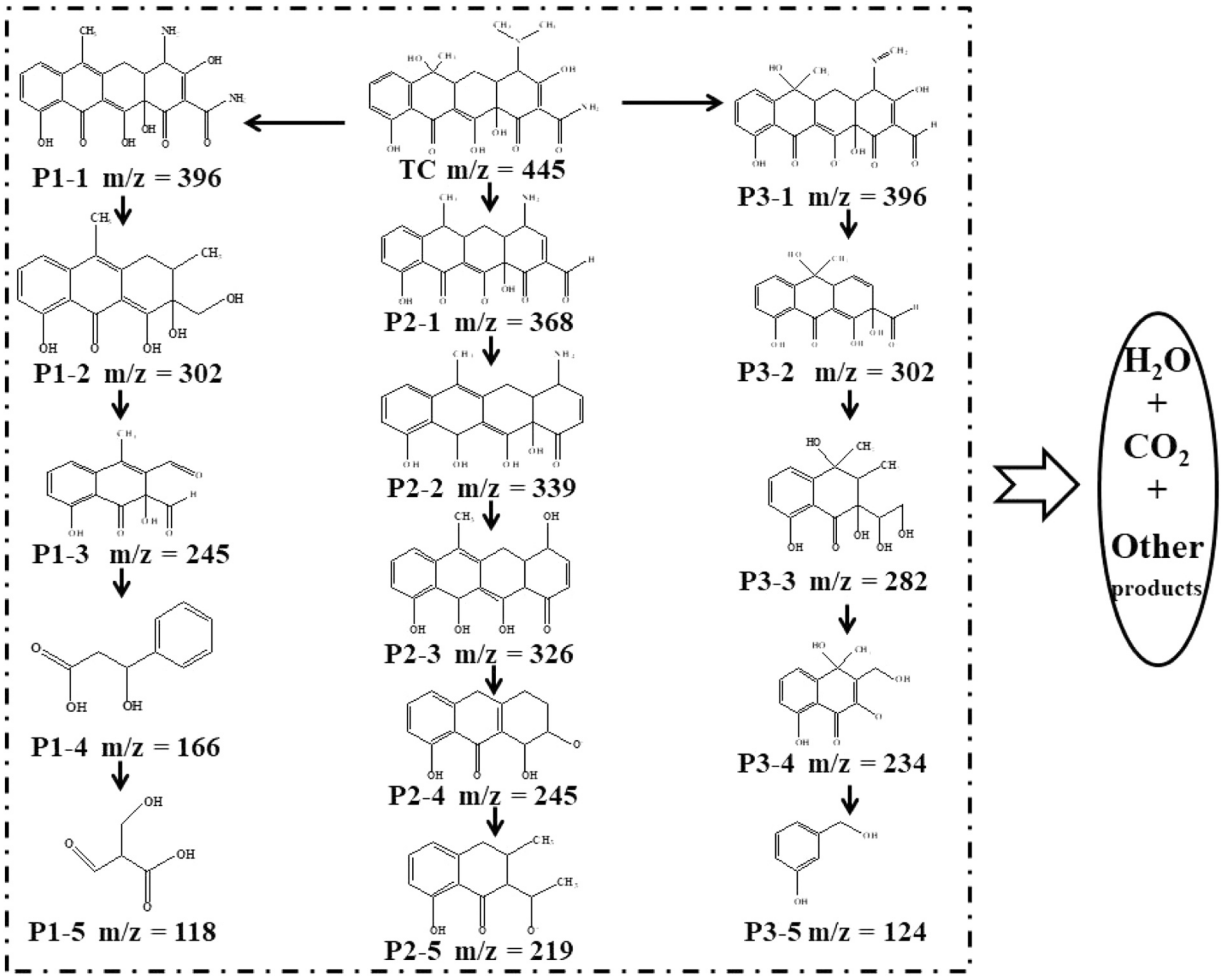

Fig. 8. Proposed pathway of tetracycline degradation in $Bi_2O_2(OH)NO_3$-$BiVO_4$ photocatalytic system.

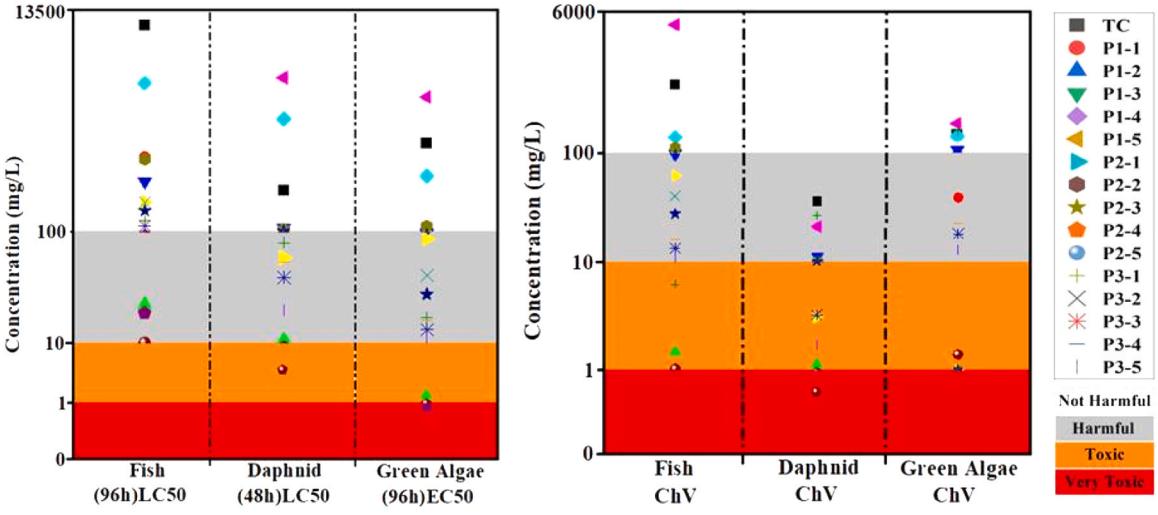

Fig. 9. Predicted toxicity of tetracycline transformation products in $Bi_2O_2(OH)NO_3$-$BiVO_4$ photocatalytic system.

and elucidate the mechanism for the degradation of tetracycline by the $Bi_2O_2(OH)NO_3$-$BiVO_4$ photocatalytic system. The quenching experiments of active species were performed by adding different scavengers, and methanol (MeOH), isopropyl alcohol (IPA) and 1,4-benzoquinone (BQ) were used as the scavenger of holes (h^+), hydroxyl radicals (·OH) and superoxide radicals ($\cdot O_2^-$). The results were displayed in Fig. 7a, which indicated that the degradation efficiencies of tetracycline were significantly inhibited by the addition of scavengers. It revealed that·OH,·O_2^-, h^+ were generated and played the most roles in the photocatalytic degradation of tetracycline. In references, h^+ and·O_2^- were mainly participated in the process of demethylationand deamination, and·OH principally lead to hydroxylation, deamidation and

ring-opening of tetracycline [49,50]. Combining with the references and band theory, the photocatalytic mechanism could be proposed in Fig. 7b. The scope of sunlight absorption can be broadened by the heterostructures of $Bi_2O_2(OH)NO_3$-$BiVO_4$, and the recombination rate of photon-generated carries (e^-/h^+) can be also postponed effectively. The photocatalytic degradation efficiencies of tetracycline could be enhanced greatly.

3.5. Degradation pathway

It reported that tetracycline was completely mineralized in a photocatalytic reaction. Usually, total organic carbon (TOC) analysis was used to investigate the mineralization efficiency. In this work, 56% of TOC removal efficiencies could be attained. It revealed that more than half of the tetracycline molecules have been completely mineralized, and the others have just been decomposed into intermediates. Therefore, an ultra-high performance liquid chromatography mass spectrometry was employed to analyze the degradation intermediates of tetracycline in the $Bi_2O_2(OH)NO_3/BiVO_4$ photocatalytic reaction system. The brief information of tetracycline and the transformation products were listed in Table 1, and three possible degradation pathways were proposed in Fig. 8.

In pathway I, tetracycline was firstly fragmented into P1–1 ($m/z = 396$) through dehydroxylation and demethylation. Secondly, P1–1 transformed into P1–2 ($m/z = 302$) after further dehydroxylation, demethylation, deamidation and ring cleavage [51]. Thirdly, P1–2 converted into P1–3 ($m/z = 245$) by demethylation, dehydroxylation, dealkylation, ring cleavage and carbonylation. Fourthly, P1–4 ($m/z = 166$) was formed by demethylation, dehydroxylation, decarbonylation, ring cleavage and hydroxylation. Fifthly, P1–5 ($m/z = 118$) was generated by dehydroxylation, carbonylation and hydroxylation. In pathway II, tetracycline was firstly decomposed into P2–1 ($m/z = 368$) through dehydroxylation and demethylation. Secondly, P2–2 ($m/z = 339$) was formed by decarbonylation. Thirdly, P2–3 ($m/z = 326$) was generated by dehydroxylation. Fourthly, P2–4 ($m/z = 245$) was transformed through demethylation, dehydroxylation and ring cleavage. Fifthly, P2–5 ($m/z = 219$) was produced by decarbonylation and ring cleavage. In pathway III, P3–1 ($m/z = 396$) was firstly obtained by removing hydroxyl group. Secondly, P3–2 ($m/z = 302$) was generated by demethylation, dehydroxylation, deamination, decarbonylation and ring cleavage. Thirdly, P3–3 ($m/z = 282$) was by further decarbonylation and ring cleavage. Fourthly, P3–4 ($m/z = 234$) was generated dehydroxylation. Fifthly, P3–5 ($m/z = 124$) was obtained by consecutive demethylation, dehydroxylation, decarbonylation and ring cleavage. Subsequently, the more small molecules could be produced and mineralized into CO_2, H_2O and NH_4^+ completely.

3.6. Toxicity prediction

The toxicity of tetracycline and the degradation intermediates were predicted by ECOSAR software, which was based on a quantitative structure-activity relationship (QSAR) model [37]. According to the structural formulas of the chemical substances, the acute toxicity and chronic toxicity was assessed by the LC_{50} of toxicity to fish, daphnia and algae. The analysis results were displayed in Fig. 9, which revealed that the acute toxicity of most tetracycline degradation products were harmless (> 100 mg/L). However, the increasing trends of the homologous chronic toxicity were also observed. Meanwhile, some of the toxicity values of the intermediates were higher than that of toxicity, which indicated that the toxicity of intermediates decreased with the photocatalytic degradation process of tetracycline. It was approximately consistent with the result of the reference, which reported that the toxicity levels showed firstly increasing and then decreasing trend [52].

4. Conclusions

In summary, the $Bi_2O_2(OH)NO_3/BiVO_4$ composite catalyst was successfully prepared by a mild and convenient hydrothermal method. A model pollutant of tetracycline was employed to investigate the activity of $Bi_2O_2(OH)NO_3/BiVO_4$ composite. The $Bi_2O_2(OH)NO_3/BiVO_4$ composite can achieve higher efficiency for tetracycline degradation, and the best degradation efficiency was 95% for 10 mg/L of tetracycline. In addition, the results of quenching experiments demonstrated that·OH,·O_2^- and h^+ were present in the $Bi_2O_2(OH)NO_3/BiVO_4$ photocatalytic system and that·OH was critical for the efficient photocatalytic degradation of tetracycline. The results of the recycling experiments revealed that the $Bi_2O_2(OH)NO_3/BiVO_4$ photocatalyst had great stability. The intermediate products of photocatalytic degradation tetracycline were detected by UPLC–MS, and the possible pathways for tetracycline degradation in the photocatalytic reaction were deduced. Base on the results of QSAR prediction, tetracycline degradation could reduce toxicity. Hence, this work supplied that new idea for the design of high-performance Bi-based composite could promote to degrade organic pollutants in aquatic systems, and some new insights of the mechanism were also provided.

CRediT authorship contribution statement

All authors of this manuscript have directly participated in planning, execution, and/or analysis of this study. The contents of this manuscript have not been copyrighted or published previously, and this manuscript is not now under consideration for publication elsewhere.

Declaration of Competing Interest

In this study, all of the authors declare no known competing financial interests, and there are not personal relationships that can be appeared to influence the work.

Data Availability

No data was used for the research described in the article.

Acknowledgements

This study was supported by the National Natural Science Foundation of China (Grant No. 22166011 and 51863004), College Students' Innovative Training Program of China (Grant No. 202110668011), Guizhou Provincial Science and Technology Projects (Grant No. ZK [2022]200 and [2020]1Y211), the Special Key Laboratory of Electrochemistry for Materials of Guizhou Province (No. QJHKYZ[2018]004).

References

[1] L. Xu, H. Zhang, P. Xiong, Q. Zhu, C. Liao, G. Jiang, Occurrence, fate, and risk assessment of typical tetracycline antibiotics in the aquatic environment: a review, Sci. Total Environ. 753 (2021), 141975.
[2] J.W. Wang, Z.P. Wang, Y.J. Cheng, L.S. Cao, F. Bai, S.Y. Yue, P.C. Xie, J. Ma, Molybdenum disulfide (MoS_2): a novel activator of peracetic acid for the degradation of sulfonamide antibiotics, Water Res 201 (2021), 117291.
[3] Y. Chen, Yi Zhou, J. Zhang, J. Li, T. Yao, A. Chen, M. Xiang, Q. Li, Z. Chen, Y. Zhou, Plasmonic Bi promotes the construction of Z-scheme heterojunction for efficient oxygen molecule activation, Chemosphere 302 (2022), 134527.
[4] Q.Q. Zhang, G.G. Ying, C.G. Pan, Y.S. Liu, J.L. Zhao, Comprehensive evaluation of antibiotics emission and fate in the river basins of China: source analysis, multimedia modeling, and linkage to bacterial resistance, Environ. Sci. Technol. 49 (2015) 6772–6782.
[5] H.L. Jiang, Q. Wang, P.H. Chen, H.T. Zheng, J.W. Shi, H.G. Shu, Y.B. Liu, Photocatalytic degradation of tetracycline by using a regenerable (Bi) BiOBr/Rgo composite, J. Clean. Prod. 339 (2022), 130771.
[6] H.F. Zhai, Y.X. Bao, S.P. Ho, Ti-based electrode materials for electrochemical sodium ion storage and removal, J. Mater. Chem. 7 (2019) 22163.
[7] X. Zhao, X. Li, X. Zhang, Y. Li, L. Weng, T. Ren, Y. Li, Bioelectrochemical removal of tetracycline from four typical soils in China: A performance assessment, Bioelectrochemistry 129 (2019) 26–33.

[8] Y. Liu, J. Li, L. Wu, D. Wan, Y. Shi, Q. He, J. Chen, Synergetic adsorption and Fenton-like degradation of tetracycline hydrochloride by magnetic spent bleach earth carbon: Insights into performance and reaction mechanism, Sci. Total Environ. 761 (2021), 143956.

[9] H. Guo, Y. Wang, X. Yao, A comprehensive insight into plasma-catalytic removal of antibiotic oxytetracycline based on graphene-TiO_2-Fe_3O_4 nanocomposites, Chem. Eng. J. (2021) 425.

[10] Y.R. Wang, D.F. Tian, W. Chu, M.R. Li, X.W. Lu, Nanoscaled magnetic $CuFe_2O_4$ as an activator of peroxymonosulfate for the degradation of antibiotics norfloxacin, Sep. Purif. Technol. 212 (2019) 536–544.

[11] W. Qiu, M. Zheng, J. Sun, Y. Tian, M. Fang, Y. Zheng, T. Zhang, C. Zheng, Photolysis of enrofloxacin, pefloxacin and sulfaquinoxaline in aqueous solution by UV/H_2O_2, UV/Fe(II), and UV/H_2O_2/Fe(II) and the toxicity of the final reaction solutions on zebrafish embryos, Sci. Total Environ. 651 (2019) 1457–1468.

[12] X.G. Li, Y.X. Guo, L.G. Yan, T. Yan, W. Song, R. Feng, Y.W. Zhao, Enhanced activation of peroxymonosulfate by ball-milled MoS_2 for degradation of tetracycline: boosting molybdenum activity by sulfur vacancies, Chem. Eng. J. 429 (2022), 132234.

[13] X. Ao, W. Sun, S. Li, C. Yang, C. Li, Z. Lu, Degradation of tetracycline by medium pressure UV-activated peroxymonosulfate process: Influencing factors, degradation pathways, and toxicity evaluation, Chem. Eng. J. 361 (2019) 1053–1062.

[14] X. Li, W. Zhu, G. Meng, C. Zhang, R. Guo, Efficiency and kinetics of conventional pollutants and tetracyclines removal in integrated vertical-flow constructed wetlands enhanced by aeration, J. Environ. Manag. 273 (2020), 111120.

[15] Z. Shi, Y. Zhang, X. Shen, et al., Fabrication of g-C_3N_4/BiOBr heterojunctions on carbon fibers as weaveable photocatalyst for degrading tetracycline hydrochloride under visible light, Chem. Eng. J. 386 (2020), 124010.

[16] X. Dai, L. Chen, Z. Li, X. Li, J. Wang, X. Hu, et al., CuS/KTa 0.75 Nb 0.25 O_3 nanocomposite utilizing solar and mechanical energy for catalytic N_2 fixation, J. Colloid Interface Sci. 603 (2021) 220–232.

[17] Z. Liang, R. Shen, P. Zhang, et al., A review on 2D MoS_2 cocatalysts in photocatalytic H_2 production, J. Mater. Sci. Technol. 56 (2020) 89–121.

[18] C. Feng, L. Tang, Y. Deng, et al., Synthesis of leaf-vein-like g-C_3N_4 with tunable band structures and charge transfer properties for selective photocatalytic H_2O_2 evolution, Adv. Funct. Mater. 30 (2020) 2001922.

[19] S. Anantharaj, S.R. Ede, K. Karthick, et al., Precision and correctness in the evaluation of electrocatalytic water splitting: revisiting activity parameters with a critical assessment, Energy Environ. Sci. 11 (2018) 744–771.

[20] Y. Wang, C. Zhang, Y. Zeng, et al., Ag and MOFs-derived hollow Co_3O_4 decorated in the 3D g-C_3N_4 for creating dual transferring channels of electrons and holes to boost CO_2 photoreduction performance, J. Colloid Interface Sci. 609 (2022) 901–909.

[21] H. Wang, X. Cai, Y. Zhang, T. Zhang, M. Chen, H. Hu, Z. Huang, J. Liang, Y. Qin, Double-template-regulated bionic mineralization for the preparation of flower-like BiOBr/carbon foam/PVP composite with enhanced stability and visible-light-driven catalytic activity, Appl. Surf. Sci. 555 (2021).

[22] H. Cai, W. Zhao, G. Xiao, et al., Process accumulated 8% efficient Cu2ZnSnS4-BiVO4 tandem cell for solar hydrogen evolution with the dynamic balance of solar energy storage and conversion, Adv. Sci. 10 (2023) 2205726.

[23] N. Mohameda, J. Safaeib, A. Ismail, et al., Boosting photocatalytic activities of $BiVO_4$ by creation of g-C_3N_4/ZnO@$BiVO_4$Heterojunction, Mater. Res. Bull. 125 (2020), 110779.

[24] R. Shen, D. Ren, Y. Ding, et al., Nanostructured CdS for efficient photocatalytic H_2 evolution: a review, Sci. China Mater. 63 (2020) 2153.

[25] J. Wang, et al., Occurrence and fate of antibiotics, antibiotic resistant genes (ARGs) and antibiotic resistant bacteria (ARB) in municipal wastewater treatment plant: an overview, Sci. Total Environ. 744 (2020), 140997.

[26] X. Chen, C. Zhen, N. Li, et al., Photochemically etching $BiVO_4$ to construct asymmetric heterojunction of $BiVO_4$/BiO_x showing efficient photoelectrochemical water splitting, Small, Methods 7 (2022) 2201611.

[27] S. Sonu, V. Sharma, P. Dutta, An overview of heterojunctioned ZnFe2O4 photocatalyst for enhanced oxidative water purification, J. Environ. Chem. Eng. 9 (2021), 105812.

[28] X. Deng, D.D. Wang, H.J. Li, W. Jiang, T.Y. Zhou, Y. Wen, B. Yu, G.B. Che, L. Wang, Boosting interfacial charge separation and photocatalytic activity of 2D/ 2D g-C_3N_4/$ZnIn_2S_4$ S-scheme heterojunction under visible light irradiation, J. Alloy. Compd. 894 (2022), 162209.

[29] L. Chi, Y. Qian, J. Guo, X. Wang, H. Arandiyan, Z. Jiang, Novel g-C_3N_4/TiO_2/PAA/PTFE ultrafiltration membrane enabling enhanced antifouling and exceptional visible-light photocatalytic self-cleaning, Catal. Today 335 (2019) 527–537.

[30] G. Alnaggar, et al., Sunlight-driven activation of peroxymonosulfate by microwave synthesized ternary MoO_3/Bi_2O_3/g-C3N4 heterostructures for boosting tetracycline hydrochloride degradation, Chemosphere 272 (2021), 129807.

[31] X. Gao, J. Niu, Y. Wang, Y. Ji, Y. Zhang, Solar photocatalytic abatement of tetracycline over phosphate oxoanion decorated Bi_2WO_6/polyimide composites, J. Hazard. Mater. 403 (2021), 123860.

[32] Y.N. Liu, J. Luo, L. Tang, C.Y. Feng, J.J. Wang, Y.C. Deng, H.Y. Liu, J.F. Yu, H. P. Feng, J.J. Wang, Origin of the enhanced reusability and electron transfer of the carbon-coated Mn_3O_4 nanocube for persulfate activation, ACS Catal. 10 (2020) 14857–14870.

[33] H. An, B. Lin, C. Xue, et al., Formation of BiOI/g-C_3N_4 nanosheet composites with high visible-light-driven photocatalytic activity, Chin. J. Catal. 39 (2018) 654–663.

[34] X. Chen, J. Zhou, Y. Chen, Degradation of tetracycline hydrochloride by coupling of photocatalysis and peroxymonosulfate oxidation processes using CuO-$BiVO_4$ heterogeneous catalyst, Process Saf. Environ. Prot. 145 (2021) 364–377.

[35] J. Zhang, M. Si, L. Jiang, X. Yuan, H. Yu, Z. Wu, Y. Li, J. Guo, Core-shell Ag@ nitrogen-doped carbon quantum dots modified $BiVO_4$ nanosheets with enhanced photocatalytic performance under Vis-NIR light: Synergism of molecular oxygen activation and surface plasmon resonance, Chem. Eng. J. 410 (2021).

[36] L.J. Yuan, Z.H. Wang, F.B. Gu, Efficient degradation of tetracycline hydrochloride by direct Z-scheme HKUST-1@ m-$BiVO_4$ catalysts with self-produced H2O2 under both dark and light, J. Environ. Chem. Eng. 10 (2022), 107964.

[37] H. Zhang, X. Wang, X. Zhao, Y. Dong, W. Wang, L. Wang, Dolomite as a low-cost peroxymonosulfate activator for the efficient degradation of tetracycline: Performance, mechanism and toxicity evolution, J. Water Process Eng. 49 (2022).

[38] T. Liu, L. Hao, L. Bai, J. Liu, Y. Zhang, N. Tian, H. Huang, Z-scheme junction $Bi_2O_2(NO_3)(OH)$/g-C_3N_4 for promoting CO_2 photoreduction, Chem. Eng. J. 429 (2022), 132268.

[39] Y. Zhou, G. Jiang, R. Wang, Photocatalytic activity of hierarchically nanoporous $BiVO_4$/TiO_2 hollow microspheres, J. Fiber Bioeng. Inform. 2 (2012) 5.

[40] G.P. Zhang, D.Y. Chen, N.J. Li, Fabrication of Bi_2MoO_6/ZnO hierarchical heterostructures with enhanced visible-light photocatalytic activity, Appl. Catal. B-Environ. 250 (2019) 313–324.

[41] L. Hao, H. Huang, Y. Guo, Multifunctional $Bi_2O_2(OH)(NO_3)$ nanosheets with {001} active exposing facets: efficient photocatalysis, dye-sensitization, and piezoelectric-catalysis, ACS Sustain. Chem. Eng. 2 (2018) 6.

[42] Q.F. Han, J.W. Pang, X. Wang, Synthesis of unique flowerlike $Bi_2O_2(OH)(NO_3)$ hierarchical microstructures with high surface area and superior photocatalytic performance, Chem. A Eur. J. 16 (2017) 23.

[43] X. Meng, Q. He, T. Song, Activation of peroxydisulfate by magnetically separable rGO $MnFe_2O_4$ toward ox oxidation of tetracycline: Efficiency, mechanism and degradation pathways, Sep. Purif. Technol. Part B 282 (2022).

[44] X. Sun, L. Huang, G. Wang, Efficient degradation of tetracycline under the conditions of high-salt and coexisting substances by magnetic $CuFe_2O_4$/g-C_3N_4 photo-Fenton process, Chemosphere 1 (2022) 308.

[45] X. Yin, X. Sun, D. Li, 2D/2D Phosphorus-doped g-C_3N_4/Bi_2WO_6 Direct Z-Scheme heterojunction photocatalytic system for tetracycline hydrochloride (TC-HCl) degradation, Int. J. Environ. Res. Public Health 22 (2022) 19.

[46] Q. Han, J. Pang, X. Wang, et al., Synthesis of unique flowerlike $Bi_2O_2(OH)(NO_3)$ hierarchical microstructures with high surface area and superior photocatalytic performance, Chem. Eur. J. 23 (2023) 3891–3897.

[47] T. Han, H. Shi, Y. Chen, et al., Facet-dependent CuO/{010}$BiVO_4$ S-scheme photocatalyst enhanced peroxymonosulfate activation for efficient norfloxacin removal, J. Mater. Sci. Technol. 3 (2023) 053.

[48] X. Yin, X. Sun, Y. Mao, et al., Synergistically enhanced photocatalytic degradation of tetracycline hydrochloride by Z-scheme heterojunction MT-$BiVO_4$ microsphere/P-doped g-C_3N_4 nanosheet composite, J. Environ. Chem. Eng. 11 (2023), 109412.

[49] X. He, T. Kai, P. Ding, Heterojunction photocatalysts for degradation of the tetracycline antibiotic: a review, Environ. Chem. Lett. 19 (6) (2021) 4563–4601.

[50] Z. Ma, L. Hu, X. Li, L. Deng, G. Fan, Y. He, A novel nano-sized MoS_2 decorated Bi_2O_3 heterojunction with enhanced photocatalytic performance for methylene blue and tetracycline degradation, Ceram. Int. 45 (13) (2019) 15824–15833.

[51] D. He, K. Zhu, J. Huang, S co-doped magnetic mesoporous carbon nanosheets for activating peroxymonosulfate to rapidly degrade tetracycline: Synergistic effect and mechanism, J. Hazard. Mater. 424 (2022).

[52] K. Gao, L. Hou, X. An, BiOBr/MXene/gC_3N_4 Z-scheme heterostructure photocatalysts mediated by oxygen vacancies and MXene quantum dots for tetracycline degradation: Process, mechanism and toxicity analysis, Appl. Catal. B: Environ. 323 (2023).